Measurement of the Beam-Helicity Asymmetry in the $p(\vec{e},e'p)\pi^0$ Reaction at the Energy of the $\Delta(1232)$ Resonance

P. Bartsch,[1] D. Baumann,[1] J. Bermuth,[2] R. Böhm,[1] K. Bohinc,[1,3] D. Bosnar,[1,*] M. Ding,[1] M. Distler,[1] D. Drechsel,[1] D. Elsner,[1] I. Ewald,[1] J. Friedrich,[1] J. M. Friedrich,[1,†] S. Grözinger,[1] S. Hedicke,[1] P. Jennewein,[1] M. Kahrau,[1] S. S. Kamalov,[1,‡] F. Klein,[1] K. W. Krygier,[1] A. Liesenfeld,[1] H. Merkel,[1] P. Merle,[1] U. Müller,[1] R. Neuhausen,[1] Th. Pospischil,[1] M. Potokar,[3] G. Rosner,[1§] H. Schmieden,[1,‖] M. Seimetz,[1] A. Süle,[1] L. Tiator,[1] A. Wagner,[1] Th. Walcher,[1] and M. Weis[1]

[1]*Institut für Kernphysik, Universität Mainz, D-55099 Mainz, Germany*
[2]*Institut für Physik, Universität Mainz, D-55099 Mainz, Germany*
[3]*Institut Jožef Stefan, University of Ljubljana, SI-1001 Ljubljana, Slovenia*

(Received 20 December 2001; published 26 March 2002)

In a $p(\vec{e},e'p)\pi^0$ out-of-plane coincidence experiment at the three-spectrometer setup of the Mainz Microtron MAMI, the beam-helicity asymmetry has been precisely measured around the energy of the $\Delta(1232)$ resonance and $Q^2 = 0.2(\mathrm{GeV}/c)^2$. The results are in disagreement with three up-to-date model calculations. This is interpreted as a lack of understanding of the nonresonant background, which in dynamical models is related to the pion cloud.

DOI: 10.1103/PhysRevLett.88.142001 PACS numbers: 13.60.Le, 13.40.–f, 14.20.Gk

Based on lepton and hadron scattering experiments the nucleon is considered as being composed of quarks and gluons. At high energies and large momentum transfers this structure can be consistently described in terms of perturbative quantum chromodynamics, because the strong coupling becomes small at the corresponding spatial scale, the regime of "asymptotic freedom." In contrast, at distances of the size of the nucleon, perturbative methods fail. Therefore, it is still an open question how QCD generates the observed "confinement" of the quarks. At the nucleon-size scale, low momentum-transfer experiments can help our understanding of the confinement mechanism by testing QCD-motivated models.

A direct consequence of the nucleon's substructure in the confinement regime is its excitation spectrum. To study the underlying internal dynamics, the prominent first excited state, the $\Delta(1232)$ resonance with spin and isospin $3/2$, has been extensively studied. In the naive quark model it emerges from the ground state by the spin flip of one of the constituent quarks, a pure $M1$ transition where one unit of angular momentum $\Delta L = 1$ is transferred. In contrast to pion scattering, electromagnetic excitation in principle accesses the positive parity $\Delta(1232)$ with both $\Delta L = 1$ and 2. While not existing in the naive quark model, quadrupole $\Delta L = 2$ transitions become possible through D-state admixtures in the baryon wave function. Those were interpreted as a deformation of the nucleon and/or the $\Delta(1232)$. In QCD-motivated constituent quark models D admixtures are generated by the color hyperfine interaction between the quarks [1–4].

However, the measured electric and scalar quadrupole to magnetic dipole ratios of $R_{\mathrm{EM}} \simeq -2.5\%$ and $R_{\mathrm{SM}} \simeq -6.5\%$ [5–11], respectively, are up to an order of magnitude larger than predicted by those models. More quadrupole strength is expected in models which emphasize the role of pions [12–16]. Through pion rescattering at the real or virtual photon $\gamma^{(*)}N\Delta$ vertex, the pion cloud is explicitly treated in the dynamical models [15,16]. A consistent decomposition into the "bare" Δ, as described in quark models, and the "dressing" by the pion cloud is performed, both for the measured quadrupole ratios and the $M1$ strength. In such models the shape is dominated by the pion cloud. From the experiment, however, no corresponding decomposition can be achieved. For an understanding of the origin of deformation it is thus important to gain insight into the purely nonresonant contributions.

In one-photon exchange approximation the fivefold differential cross section of pion electroproduction,

$$\frac{d^5\sigma}{dE_e\, d\Omega_e\, d\Omega_\pi^{\mathrm{cm}}} = \Gamma \frac{d^2\sigma_v}{d\Omega_\pi^{\mathrm{cm}}}, \tag{1}$$

factorizes into the virtual photon flux,

$$\Gamma = \frac{\alpha}{2\pi^2} \frac{E'}{E} \frac{k_\gamma}{Q^2} \frac{1}{1-\epsilon}, \tag{2}$$

and the virtual photon cm cross section, $d^2\sigma_v/d\Omega_\pi^{\mathrm{cm}}$. α denotes the fine structure constant, $k_\gamma = (W^2 - m_p^2)/2m_p$ the real photon equivalent laboratory energy for the excitation of the target with mass m_p to the cm energy W, and $\epsilon = [1 + (2|\vec{q}|^2/Q^2)\tan^2\frac{\vartheta_e}{2}]^{-1}$ the photon polarization parameter. $Q^2 = |\vec{q}|^2 - \omega^2$ is the squared four-momentum transfer, $\vec{q}$ and ω are the three-momentum and energy transfer, respectively, and E, E', and ϑ_e the incoming and outgoing electron energy, and the electron scattering angle in the laboratory frame.

Without target or recoil polarization, the virtual photon cross section is given by [17]

$$\frac{d^2\sigma_v}{d\Omega_\pi^{\rm cm}} = \lambda[R_T + \epsilon_L R_L + \sqrt{2\epsilon_L(1+\epsilon)}\, R_{LT}\cos\Phi + \epsilon R_{TT}\cos 2\Phi + P_e\sqrt{2\epsilon_L(1-\epsilon)}\, R_{LT'}\sin\Phi]. \quad (3)$$

The factor $\lambda = |\vec{p}_\pi^{\rm cm}|/k_\gamma^{\rm cm}$ is determined by the pion cm momentum $\vec{p}_\pi^{\rm cm}$ and $k_\gamma^{\rm cm} = (m_p/W)k_\gamma$. The structure functions R_i describe the response of the hadronic system to the various polarization states of the photon field, which are described by the transverse and longitudinal polarization, ϵ and $\epsilon_L = \frac{Q^2}{\omega_{\rm cm}^2}\epsilon$, respectively, and by the longitudinal electron polarization, P_e. The tilting angle between the electron scattering plane and the reaction plane is denoted by Φ, where $\Phi = 0°$ and $180°$ correspond to pions ejected in the electron scattering plane, and $\Phi = 90°$ and $270°$ perpendicularly to the scattering plane.

High sensitivity to $R_{\rm EM}$ and $R_{\rm SM}$ is obtained through the pion P-wave interferences $\mathrm{Re}\{E_{1+}^* M_{1+}\}$ and $\mathrm{Re}\{S_{1+}^* M_{1+}\}$ occurring in R_{TT} and R_{LT}, respectively. These interferences can also be accessed by measuring the recoil polarization in the $p(\vec{e}, e'\vec{p})\pi^0$ reaction [18]. For parallel kinematics the beam-helicity independent polarization component, P_y, reads in S and P-wave M_{1+}-dominance approximation, which is used only for simplicity,

$$\sigma_0 P_y = -c_+\tilde{\lambda}\,\mathrm{Im}\{(4S_{1+} + S_{1-} - S_{0+})^* M_{1+}\}. \quad (4)$$

σ_0 denotes the unpolarized cross section, $c_\pm = \sqrt{2\epsilon_L(1\pm\epsilon)}$ and $\tilde{\lambda} = \omega_{\rm cm}/|\vec{q}_{\rm cm}|$. The experimental results for P_y are not well reproduced by model calculations [8,19].

It is unclear whether this disagreement originates from higher resonances, like the Roper N(1440) which couples to the S_{1-} partial wave, or to nonresonant contributions. Moreover, a model independent relation between the transverse and longitudinal recoil polarization components [20] is possibly violated by the MAMI experiment [8].

In the same approximation the structure function $R_{LT'}$ has a similar structure as $\sigma_0 P_y$:

$$R_{LT'} = -\sin\Theta\,\tilde{\lambda}\,\mathrm{Im}\{(6\cos\Theta S_{1+} + S_{0+})^* M_{1+}\}. \quad (5)$$

At the resonance energy, where the isospin-3/2 part of $\mathrm{Re}M_{1+}$ crosses zero, $R_{LT'}$ is exclusively sensitive to the nonresonant scalar amplitudes. The measurement of

$$\rho_{LT'} = \frac{c_- R_{LT'}\sin\Phi}{R_T + \epsilon_L R_L + c_+ R_{LT}\cos\Phi + \epsilon R_{TT}\cos 2\Phi} \quad (6)$$

is thus expected to shed more light on the above discrepancies and the origin of nucleon deformation. $\rho_{LT'}$ is experimentally easy to access as an asymmetry with regard to the helicity reversal of the electron beam, once out-of-plane proton detection is provided [21].

The $p(\vec{e}, e'p)\pi^0$ experiment was carried out at the three-spectrometer facility [22] of the A1 collaboration at the Mainz Microtron MAMI. A typically 6 μA electron beam with 80% polarization impinged on a 5 cm long liquid hydrogen target cell made of a 10 μm Havar foil. Longitudinal beam polarization at the target was obtained by fine tuning the beam energy to $E = 854.5$ MeV. The beam polarization was measured on a daily basis with a Møller polarimeter [23] located 15 m straight upstream of the target. The scattered electrons were detected in spectrometer A of the three-spectrometer setup, which was set to an angle of 44.5° and a central momentum of 408 MeV/c.

For the coincident proton detection the out-of-plane capability of spectrometer B was used. It was set to $-26.9°$ in the horizontal plane and then tilted out of plane in three different settings of $\Theta_{\rm OOP} = 2$, 7, and 10°.

Both spectrometers are equipped with two double planes of vertical drift chambers for particle tracking, and two segmented planes of fast plastic scintillators for particle identification via dE/dx and timing measurements. The standard detector packages are completed by a threshold gas Cherenkov detector for $e^\pm$ identification. In spectrometer A this device was replaced by the focal plane proton polarimeter [24] for other experiments.

Figure 1 (left) shows the coincidence time between spectrometers A (start) and B (stop). Two prompt peaks are obtained on a tiny random background. The left peak is associated with $p(e,\pi^- p)\pi^+ e'$ double pion production, where the π^- is detected in spectrometer A instead of the scattered electron. The right peak is well separated. It represents the true $e'p$ coincidences of the $p(\vec{e}, e'p)\pi^0$ reaction. A coincidence time resolution of 0.8 ns FWHM results in a true to random ratio of 76:1.

The final state π^0 remains unobserved. Because of the complete kinematics, the $p(\vec{e}, e'p)\pi^0$ reaction can be reconstructed via the missing mass. Figure 1 (right) shows a clear peak of $\simeq$4.5 MeV/c^2 FWHM at the π^0 mass. The strength at higher missing mass is due to random background, which still is included, radiative processes, and misidentified double pion production. The latter contribution is marked by the dark shaded areas. The light shaded areas are related to true coincidences. A cut of -5–100 MeV/c^2 around the π^0 mass selects the

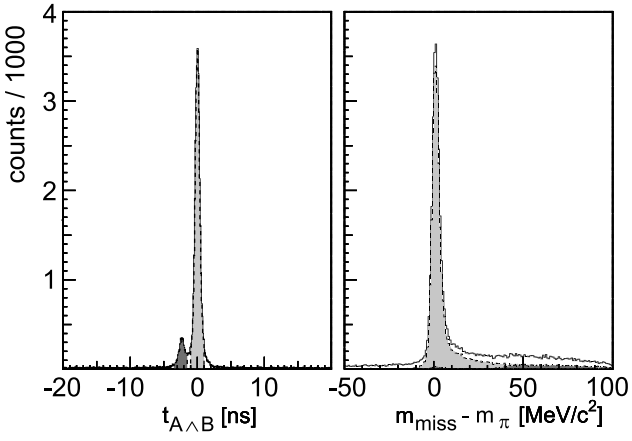

FIG. 1. Left: Coincidence time spectrum between spectrometers A and B. Right: Missing mass for the $p(\vec{e}, e'p)X$ reaction. The (hardly visible) dark shaded areas are due to misidentified double pion production, the light shaded areas represent the true $e'p$ coincidences. See text for discussion.

$p(e, e'p)\pi^0$ reaction. There is less than 0.1% background remaining after random coincidences are subtracted.

The beam-helicity asymmetry $\rho_{LT'}^{\exp} = \frac{1}{P}(N^+ - N^-)/(N^+ + N^-)e$ is constructed from the numbers of events, $N^{\pm}$, selected for beam helicity + and −, respectively. Results for individual bins over the total accepted phase space, $W = 1180$–1290 MeV, $Q^2 = 0.14°$–$0.26°$ $(\mathrm{GeV}/c)^2$, $\epsilon = 0.536°$–$0.664°$, and $\Theta_\pi^{\mathrm{cm}} = 130°$–$180°$, were obtained, with a varying azimuthal acceptance of $\Delta\Phi = 20°$–$360°$ depending on Θ_π^{cm}. The stability of the results was checked by varying the cuts in coincidence time and missing mass. The latter produced a systematic variation of $\rho_{LT'}$ which, however, could be entirely attributed to the corresponding variation in the nonindependent other kinematic variables. The remaining effect of radiative processes is thus estimated to <1%.

The systematic errors of the asymmetry measurement are dominated by the uncertainty of the beam polarization. Individual beam polarization measurements achieve 2% accuracy when statistical and systematical errors are added in quadrature. Undetected fluctuations of polarization are accounted for by an additional 2% error, which is estimated from long term stability measurements during G_E^n experiments. Helicity-specific luminosity fluctuations are smaller than 0.5%.

For the compilation of the results in Table I and the presentation in Fig. 2, $\rho_{LT'}(W, Q^2, \epsilon, \Theta_\pi^{\mathrm{cm}}, \Phi)$ is projected to nominal kinematics ($W = 1232$ MeV, $Q^2 = 0.2$ $(\mathrm{GeV}/c)^2$, $\epsilon = 0.6$, $\Theta_\pi^{\mathrm{cm}} = 155°$, $\Phi = 270°$) using the unitary isobar model MAID2000 [25]:

$$\rho_{LT'} = \frac{\rho_{LT'}^{\mathrm{MAID}}(\mathrm{nom.kin.})}{\rho_{LT'}^{\mathrm{MAID}}(W, Q^2, \epsilon, \Theta_\pi^{\mathrm{cm}}, \Phi)} \times \rho_{LT'}^{\exp}(W, Q^2, \epsilon, \Theta_\pi^{\mathrm{cm}}, \Phi). \quad (7)$$

This is done simultaneously for all except the respective running variables. An additional systematic error of 1.8% due to the projection procedure is estimated by a ±5% variation of the M_{1+} multipole in MAID and a ±50% variation of the other S- and P-wave multipoles. Quadratic addition of the individual contributions yields a total relative systematic error of <3.4%.

The results are compared to MAID2000 and the dynamical models of Kamalov and Yang [15] and Sato and Lee [16]. Very similarly to the normal component P_y of the recoil proton polarization in the $p(\vec{e}, e'\vec{p})\pi^0$ reaction [8,19] MAID overestimates the magnitude of the asymmetry by one third. The appropriately scaled MAID curve describes the differential dependencies of $\rho_{LT'}$ very well. This is important for the projection to nominal kinematics [Eq. (7)]. While the dynamical model of Kamalov-Yang overestimates $\rho_{LT'}$ in magnitude as well, the Sato-Lee model underestimates this quantity.

At present, it therefore appears that neither of the models is capable of reproducing the measured $\rho_{LT'}$. This may be related to the strength of S_{0+}. MAID2000 simultaneously describes P_y [8] and the angular distribution of $\rho_{LT'}$ (Fig. 2, top), if the $\mathrm{Re}S_{0+}$ strength is artificially reduced by approximately 60%. Such contributions can be obtained from pion loops and/or dispersion integrals from higher S-wave resonances. The nonresonant contributions of higher partial waves are more reliably described by Born terms. Around $W = 1232$ MeV, significant non-Born contributions are almost excluded by experiment [11,26]. The Kamalov-Yang model reproduces P_y pretty well, but fails at the same time for $\rho_{LT'}$. It seems that pion cloud effects are not yet consistently included in the dynamical models. A consistent understanding of the nonresonant background is an important issue already in the case of the $\Delta(1232)$ resonance, where this might — but does not necessarily — affect the extraction of resonance properties from π^0 electroproduction experiments [27]. It will be mandatory for the investigation of higher, weak and overlapping, resonances.

In summary, for the first time a measurement of the $\rho_{LT'}$ helicity asymmetry in a $p(\vec{e}, e'p)\pi^0$ out-of-plane

TABLE I. Results for the beam-helicity asymmetry $\rho_{LT'}$ with statistical errors. Except for the respective running variable a projection to nominal kinematics has been performed using MAID2000 (see text).

Θ_π^{cm} (deg)	$\rho_{LT'}$	W (MeV)	$\rho_{LT'}$
123.3	−0.0427 ± 0.0186	1178	−0.0554 ± 0.0050
130.0	−0.0469 ± 0.0061	1192	−0.0573 ± 0.0031
136.6	−0.0576 ± 0.0032	1205	−0.0635 ± 0.0024
143.3	−0.0652 ± 0.0022	1218	−0.0601 ± 0.0021
150.0	−0.0681 ± 0.0020	1232	−0.0683 ± 0.0023
156.6	−0.0681 ± 0.0020	1245	−0.0724 ± 0.0026
163.3	−0.0627 ± 0.0023	1258	−0.0800 ± 0.0032
170.0	−0.0465 ± 0.0030	1272	−0.0742 ± 0.0045
176.6	−0.0179 ± 0.0041	1285	−0.0701 ± 0.0118
Q^2 (GeV^2/c^2)		Q^2 (GeV^2/c^2)	
0.172	−0.0638 ± 0.0034	0.228	−0.0683 ± 0.0021
0.200	−0.0682 ± 0.0019	0.256	−0.0704 ± 0.0047

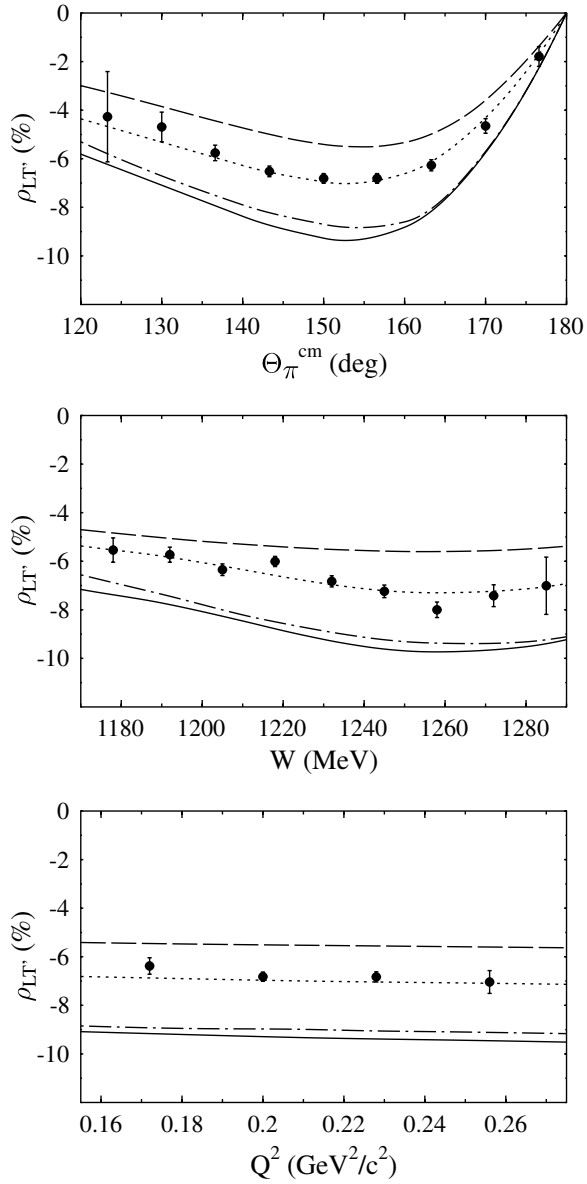

FIG. 2. Results for $\rho_{LT'}$ as a function of $\Theta_\pi^{\rm cm}$ (top), W (middle), and Q^2 (bottom). The full curve represents the MAID calculation [25], the dotted curve is MAID scaled by a factor 0.75. The dashed and dash-dotted curves are the results of the dynamical models of Sato-Lee [16] and Kamalov-Yang [15], respectively. Errors are purely statistical.

coincidence experiment is reported. The high statistical accuracy is complemented by a small relative systematic error which is estimated to be $<3.4\%$. Neither of three up-to-date model calculations is capable of quantitatively reproducing the observed asymmetries. From the failure of the dynamical models it is concluded that pion cloud effects are not yet sufficiently well understood.

We are indebted to K.-H. Kaiser and K. Aulenbacher and their staff for providing the excellent polarized beam. We thank T. Sato and T.-S. H. Lee for providing us with their calculations. Helpful discussions with R. Beck are gratefully acknowledged. This work was supported in part by the Deutsche Forschungsgemeinschaft (SFB443) and the federal state of Rheinland-Pfalz.

*Permanent address: Department of Physics, University of Zagreb, Zagreb, Croatia.
†Present address: Physik Department E18, TU München, Germany.
‡Permanent address: Laboratory for Theoretical Physics, JINR Dubna, Dubna, Russia.
§Present address: Department of Physics and Astronomy, University of Glasgow, Glasgow, United Kingdom.
‖Corresponding author.
Present address: Physikalisches Institut, Universität Bonn, Bonn, Germany.
Email address: schmieden@physik.uni-bonn.de

[1] A. de Rújula, H. Georgi, and S. L. Glashow, Phys. Rev. D **12**, 147 (1975).
[2] N. Isgur, G. Karl, and R. Koniuk, Phys. Rev. D **25**, 2394 (1982).
[3] S. S. Gershtein and G. V. Dzhikiya, Sov. J. Nucl. Phys. **34**, 870 (1982).
[4] D. Drechsel and M. M. Giannini, Phys. Lett. **143B**, 329 (1984).
[5] R. Beck *et al.,* Phys. Rev. Lett. **78**, 606 (1997).
[6] G. Blanpied *et al.,* Phys. Rev. Lett. **79**, 4337 (1997).
[7] V. V. Frolov *et al.,* Phys. Rev. Lett. **82**, 45 (1999).
[8] Th. Pospischil *et al.,* Phys. Rev. Lett. **86**, 2959 (2001).
[9] C. Mertz *et al.,* Phys. Rev. Lett. **86**, 2963 (2001).
[10] R. W. Gothe, Prog. Part. Nucl. Phys. **44**, 185 (2000).
[11] K. Joo *et al.,* nucl-ex/0110007v2.
[12] G. C. Gellas *et al.,* Phys. Rev. D **60**, 054022 (1999).
[13] A. Silva *et al.,* Nucl. Phys. **A675**, 637 (2000).
[14] A. J. Buchmann *et al.,* Phys. Rev. C **58**, 2478 (1998).
[15] S. S. Kamalov and S. N. Yang, Phys. Rev. Lett. **83**, 4494 (1999).
[16] T. Sato and T.-S. H. Lee, Phys. Rev. C **63**, 055201 (2001).
[17] D. Drechsel and L. Tiator, J. Phys. G **18**, 449 (1992).
[18] H. Schmieden, Eur. Phys. J. A **1**, 427 (1998).
[19] G. Warren *et al.,* Phys. Rev. C **58**, 3722 (1998).
[20] H. Schmieden and L. Tiator, Eur. Phys. J. A **8**, 15 (2000).
[21] C. Papanicolas, in *Proceedings of NSTAR2001,* edited by D. Drechsel and L. Tiator (World Scientific, Singapore, 2001), p. 11.
[22] K. I. Blomqvist *et al.,* Nucl. Instrum. Methods Phys. Res., Sect. A **403**, 263 (1998).
[23] P. Bartsch, doctoral thesis, Mainz, 2002; P. Bartsch *et al.* (to be published).
[24] Th. Pospischil *et al.,* Nucl. Instrum. Methods Phys. Res., Sect. A (to be published).
[25] D. Drechsel, O. Hanstein, S. S. Kamalov, and L. Tiator, Nucl. Phys. A **645**, 145 (1999); http://www.kph.uni-mainz.de/MAID/maid2000/
[26] R. Beck *et al.,* Phys. Rev. C **61**, 035204 (2000).
[27] H. Schmieden, in Ref. [21], p. 27.